

Optimization of Wood Welding Parameters for Australian Hardwood Species

Benoit Belleville,^{a,*} Siham Amirou,^b Antonio Pizzi,^c and Barbara Ozarska^a

Optimal linear wood welding parameters along the end-grain-to-end-grain faces were determined for *Eucalyptus saligna*, *Eucalyptus pilularis*, and *Corymbia maculata*. Joints made using *Eucalyptus saligna* showed a significant interaction between welding time (WT), amplitude (WA), and pressure (WP). A preheating phase of 3 s at 0.4 MPa WP and 0.75 mm WA coupled with a WT of 2 s at 2.0 MPa WP and 1.5 mm WA provided the best shear strength results of 5.1 MPa. Joints made using *Eucalyptus pilularis* and *Corymbia maculata* snapped once the holding pressure was removed, suggesting that end-grain-to-end-grain welded fibers cannot withstand the thermal stresses generated when the surface to be welded is too small (e.g., 13.5 cm²). However, grain orientation had a significant effect on the weld mechanical properties, as very strong edge-grain-to-edge-grain joints were produced with *Eucalyptus pilularis* and *Corymbia maculata* (9.5 and 6.2 MPa, respectively). The joints made of *Eucalyptus saligna* also showed significant improvement (7.3 MPa). Energy efficient combinations were usually those involving low WA and short WT, as WP had a marginal effect on energy consumption during the welding process.

Keywords: Linear wood welding; *Eucalyptus saligna*; *Eucalyptus pilularis*; *Corymbia maculata*; End-grain butt joint; Edge-grain-to-edge-grain faces joints

Contact information: a: The University of Melbourne, Faculty of Science, School of Ecosystem and Forest Sciences, Burnley campus, 500 Yarra Boulevard, Richmond, Victoria, Australia, 3121; b: King Abdulaziz University, Department of Physics, Jeddah, Saudi Arabia; c: LERMAB, University of Lorraine, 27 rue Philippe Seguin, Epinal, France, 88051; * Corresponding author: benoit.belleville@unimelb.edu.au

INTRODUCTION

Wood welding has the potential of being a fast and cost-effective alternative to gluing wood (Martins *et al.* 2013; Zhang *et al.* 2014). The technique consists in assembling solid wood pieces by mechanical friction to generate heat, which induces the lignin to soften and the wood to weld. Preliminary results suggest that Australian wood species are ideal for end-grain butt joints welding because of their high density (Mansouri *et al.* 2010). However, not much applied research has been carried out to develop a production process or useful products utilizing these materials. In the current stage of development, the welding process also creates a fine black burn line at the weld, which could be considered non-aesthetic for indoor wood products. Optimizing wood welding parameters and reducing the charring line to a point where it would not have a visual impact without affecting the bonding properties would be ideal. Wood welding could, therefore, be used for eco-concept indoor applications such as flooring overlay.

The aim of the present work was to bring this innovative technique to an efficient manufacturing process level and to produce high-value wood products that meet the criteria of customers and building standards. The specific objectives of the present study

were (1) to assess the linear wood welding potential of three commercial Australian wood species for the production of end-grain butt joints, (2) to determine the optimal end-grain welding parameters, *i.e.* time, amplitude and pressure, for each species from the joint shear strength and energy consumption during the welding process and (3) to assess the impact of fiber orientation on the joint mechanical properties by comparing with edge-grain-to-edge-grain faces joints (*i.e.* laminated joints).

EXPERIMENTAL

Wood species

Three hardwood species were selected because of their availability as plantation timbers and their high potential and commercial value: *Eucalyptus saligna* (air dry density of 784 kg m⁻³ at 12 % MC), *Eucalyptus pilularis* (925 kg m⁻³), and *Corymbia maculata* (965 kg m⁻³). All three species are diffuse-porous sharing similar anatomical features such as procumbent ray cells with 4 to 12 rays per mm and a ray width of 1 to 3 cells (InsideWood 2004).

Preliminary trials

A factorial plan was used to evaluate a wide range of welding pressures (WP), vibrational or welding amplitudes (WA), and welding times (WT) for the production of end-grain butt joints using a linear vibration welding machine (KLN Ultraschall LVW 2361, Annemasse, France). The welding sequence was divided into three phases: 1) the preheating phase to progressively ramp up WP and WA; 2) the welding phase where WP and WA were maintained for a specific WT; and 3) the cooling phase where WP was maintained on the welded specimen with no vibrational movement. The preheating phase was further divided into two substeps consisting of 1 s at 0.2 MPa WP and 1.0 mm WA followed by 1 s at 0.2 MPa and 2.0 mm WA. For the welding phase, four WTs (2, 4, 6, and 8 s) and three WPs (1.5, 3.0, and 4.5 MPa) were considered. A cooling phase of 60 s at 2.0 MPa was considered for all combinations. Two wooden pieces each measuring 15 × 90 × 40 mm³ were welded along the end-grain-to-end-grain faces at a frequency of 150 Hz. Two welded specimens 15 × 90 × 80 mm³ were prepared per combination and species. The parameters proposed by Mansouri *et al.* (2010, Table 1) for high density eucalypts were also included for comparison purposes.

Table 1. Welding Parameters Used by Mansouri *et al.* (2010) for End-Grain Butt Joints of High Density Eucalyptus Wood

Species	Welding Time* (s)	Welding Pressure* (MPa)	Welding Amplitude* (mm)	Shear Strength (MPa)
<i>Eucalyptus saligna</i>	6 (1/1/4/5)	0.25/0.25/1.75/2.0	1/2/2/0	6.6
<i>Corymbia maculata</i>	8 (1/1/6/5)	0.25/0.25/1.75/2.0	1/2/2/0	8.6
<i>Eucalyptus pilularis</i>	6 (1/1/4/5)	0.25/0.25/1.75/2.0	1/2/2/0	5.3

* A welding sequence consisted in two preheating phase substeps to ramp up welding amplitude, the welding phase and the cooling phase.

Prior to testing, the welded specimens were placed in a conditioning room at 23 °C and 65% relative humidity until a constant mass was achieved. The welded specimens were then cut to prepare block shear samples (Fig. 1). A cut perpendicular and down to the weldline was made on each side to provide an effective welded area of $15 \times 40 \text{ mm}^2$. Shear strength testing was conducted using a universal testing machine (Instron model 4467, Norwood, MA, USA) by compression loading at a rate of 2 mm/s (Fig. 2).

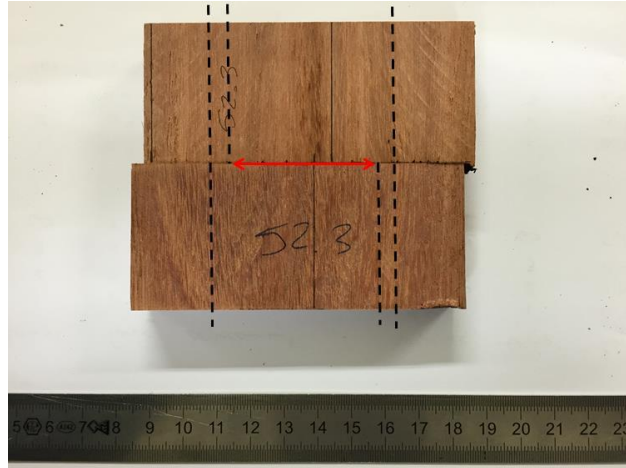


Fig. 1. A welded *Eucalyptus saligna* specimen ready to be cut (dotted lines) to prepare a block shear sample with a welded area of $15 \times 40 \text{ mm}^2$ (red arrow)



Fig. 2. Shear strength test setup

Main testing trials

From the mechanical testing results of the preliminary trials the following elements were considered for main optimization trials:

- Focusing on the lower range of assessed WPs, application of 3.0 MPa and higher provided lower mechanical properties, probably as a result of excessive charring;
- Focusing on the lower range of assessed WT during the welding phase, 4 s and longer generated excessive charring and smoke while providing lower mechanical properties;

- Reducing WA was done during both the preheating and welding phases from 1 mm and 2 mm to 0.75 mm and 1.50 mm, respectively, in an attempt to limit fiber degradation during friction welding;
- Extending the preheating phase by 1 s and increasing the pressing pressure from 0.2 to 0.4 MPa was carried out to shorten the exposure to high pressure and amplitude during the welding phase;
- The WP was increased during the cooling phase from 2.0 to 3.7 MPa, as recommended by Martins *et al.* (2013) who investigated a similar species, as all welded samples made from *Eucalyptus pilularis* and *Corymbia maculata* snapped by themselves within minutes after removing the holding pressure.

Ten welded specimens per combination and species were prepared and tested as described above. During the welding process the energy consumption was also measured using an integrated energy control acquisition system (KLN Ultraschall LVW 2361, Annemasse, France). Edge-grain-to-edge-grain faces joints were prepared using welding parameters showing the best potential for end-grain jointing and combinations adapted from the literature. Again, 10 welded specimens per combination and species were prepared and tested to assess the impact of fiber orientation on the mechanical properties of wood welded joints. Test results were subjected to analyses of variance (ANOVA) using Minitab statistical software (v16.1.0, Minitab, State College, PA, USA).

RESULTS AND DISCUSSION

As observed during the preliminary trials, all *Eucalyptus pilularis* and *Corymbia maculata* welded samples snapped shortly after removing the holding pressure. As all three tested species shared similar anatomical features, a higher density could have affected the strength of the welded joint, as observed in rotational wood welding (Belleville *et al.* 2016). Another potential explanation of the observed differences could be the presence of vessels in a diagonal and/or radial pattern in the case of *Eucalyptus pilularis* and *Corymbia maculata*. Interestingly, the present experimental plan was identical to that of Mansouri *et al.* (2010) except for the welded surface, which was much smaller in the present case (*i.e.*, $180 \times 20 \text{ mm}^2$ versus $90 \times 15 \text{ mm}^2$). In metal welding both the solidification rate (Zhou and Tsai 2007) and weld pool geometry (Haboudou *et al.* 2003) influence the porosity formation and consequently affect the quality of a joint. As the matrix of a molten material solidifies, stresses are generated at the center, resulting in the formation of porosity and ultimately solidification cracking if the weld has insufficient strength to withstand it (TWI 1999). The weld becomes prone to cracking as stresses through thermal contraction build up, similarly to springback in the case of particleboards.

Mansouri *et al.* (2010) observed cracks in welded butt joints and attributed them to testing and sawing. However, it is likely that the observed cracks could have been generated during the welding stage but were small enough to withstand the thermal stresses generated in the joints. The welded surfaces used in each study were different, which could have potentially affected the solidification rate and consequently the stresses generated, creating a weak zone in the weld. Zhang *et al.* (2014) also found cracks in joints of *Borassus flabellifer* if the WP was higher than 2 MPa, which affected the

homogeneity of the weldline. The mechanical performance of a joint is strongly correlated with the density profile of the weld, as a narrower and homogeneous density profile usually provides better performance. As explained by Leonard and Lockyer (2003), the formation of weld flaws (*e.g.*, porosity and solidification cracking) are inherent in most material joining processes, and successful and reproducible welds may only be produced when operating within specific process limits. Thus, the welded surface in the present study was ultimately too small to withstand the level of stress generated, and as a result, *Eucalyptus pilularis* and *Corymbia maculata* were not able to provide effective end-grain welds.

In the case of end-grain joints made from *Eucalyptus saligna*, the results of the ANOVA showed a triple interaction between WT, WA, and WP during the welding phase (F -value = 5.11, Table 2). The results were in accordance with those of Gfeller *et al.* (2003), although those authors made no differentiation between WP during the preheating or welding phases. In the present study, a 2.0 MPa WP during the welding phase provided significantly better results (F -values = 13.90), where a 0.2 or 0.4 MPa WP during the preheating phase had no effect on the shear strength of the joints. The optimized WP during welding was also slightly higher than what was proposed by Mansouri *et al.* (2010) for the same species.

Table 2. ANOVA (F -values) Results for End-Grain Joints Made from *Eucalyptus saligna* as a Function of Welding Parameters

Source of Variation	F -value	Pr > F
Welding Time (WT)	4.55	0.037
Welding Pressure Preheating Phase (WP1)	0.30	0.585
Welding Pressure Welding Phase (WP2)	13.90	0.000
Welding Amplitude (WA)	6.97	0.010
WT x WP1	0.25	0.617
WT x WP2	3.72	0.058
WT x WA	0.00	0.971
WP1 x WP2	0.91	0.344
WP1 x WA	0.91	0.344
WP2 x WA	12.69	0.001
WT x WP1 x WP2	1.77	0.189
WT x WP1 x WA	0.11	0.747
WT x WP2 x WA	5.11	0.027
WP1 x WP2 x WA	1.88	0.175
WT x WP1 x WP2 x WA	0.38	0.542

A WT of 2 s (5 s total when including the preheating phase of 3 s) provided significantly better mechanical properties using a Tukey grouping method with 95.0% confidence intervals. Transferring one second from the welding phase to the second step of the preheating phase also proved to enhance the weld strength. Reducing the WA during both the preheating and welding phases from 1 mm and 2 mm to 0.75 mm and 1.50 mm, respectively, also improved the weld mechanical properties significantly (F -value = 6.97). The results tend to confirm that achieving a strong bond between the materials is dependent on creating a right balance between time and exposure conditions to friction-induced high temperature.

Two combinations of parameters provided higher results than the other tested combinations. The first one was a welding time of 6 s combined with a 1/2/2 mm WA,

providing an average shear strength result of 5.30 ± 0.90 MPa. However, such a combination generated high variation between samples while consuming the second most energy out of all tested combinations at 2232 J per welded sample (Table 3). The second combination was a welding time of 5 s combined with a 0.75/1.5/1.5 mm WA at 5.14 ± 0.45 MPa. This combination required significantly less energy than the other combination at 1774 J per sample. The most energy-efficient combinations were usually those using a low WA and short WT, while WP only had a marginal effect on energy consumption. Interestingly, energy consumption appears to be a valuable optimization and quality control tool to assess the quality of a produced weld, as individual measurements seemed to strongly correlate with mechanical results.

Table 3. Shear Strength Properties and Energy Consumption per Combination of Welding Parameters, Species, and Type of Joint

Species	Welding Time* (s)	Welding Pressure* (MPa)	Welding Amplitude* (mm)	Shear Strength** (MPa)	Energy Consumption** (J)
End-Grain-to-End-Grain Joint					
<i>E. saligna</i>	5 (1/2/2/60)	0.4/0.4/1.0/3.7	0.75/1.5/1.5/0	4.93±0.51 ^{def}	1787±39 ^g
<i>E. saligna</i>	5 (1/2/2/60)	0.2/0.2/1.0/3.7	0.75/1.5/1.5/0	4.68±1.05 ^{efg}	1795±39 ^g
<i>E. saligna</i>	5 (1/2/2/60)	0.4/0.4/1.0/3.7	1/2/2/0	3.01±1.48 ^{ghi}	1879±28 ^{ef}
<i>E. saligna</i>	5 (1/2/2/60)	0.2/0.2/1.0/3.7	1/2/2/0	4.51±0.94 ^{efg}	1897±25 ^e
<i>E. saligna</i>	6 (1/2/3/60)	0.4/0.4/1.0/3.7	0.75/1.5/1.5/0	4.43±0.64 ^{efg}	2050±49 ^{cd}
<i>E. saligna</i>	6 (1/2/3/60)	0.2/0.2/1.0/3.7	0.75/1.5/1.5/0	4.24±0.55 ^{fg}	1998±52 ^{cd}
<i>E. saligna</i>	6 (1/2/3/60)	0.4/0.4/1.0/3.7	1/2/2/0	1.79±1.65 ⁱ	2141±133 ^b
<i>E. saligna</i>	6 (1/2/3/60)	0.2/0.2/1.0/3.7	1/2/2/0	2.92±1.53 ^{hi}	2248±49 ^b
<i>E. saligna</i>	5 (1/2/2/60)	0.4/0.4/2.0/3.7	0.75/1.5/1.5/0	5.14±0.45 ^{def}	1774±37 ^g
<i>E. saligna</i>	5 (1/2/2/60)	0.2/0.2/2.0/3.7	0.75/1.5/1.5/0	4.73±0.37 ^{efg}	1799±58 ^g
<i>E. saligna</i>	5 (1/2/2/60)	0.4/0.4/2.0/3.7	1/2/2/0	4.98±0.21 ^{def}	1834±130 ^{fg}
<i>E. saligna</i>	5 (1/2/2/60)	0.2/0.2/2.0/3.7	1/2/2/0	4.20±2.18 ^{fg}	1891±23 ^e
<i>E. saligna</i>	6 (1/2/3/60)	0.4/0.4/2.0/3.7	0.75/1.5/1.5/0	4.08±0.42 ^{fgh}	2063±24 ^c
<i>E. saligna</i>	6 (1/2/3/60)	0.2/0.2/2.0/3.7	0.75/1.5/1.5/0	4.49±0.26 ^{efg}	2003±40 ^{cd}
<i>E. saligna</i>	6 (1/2/3/60)	0.4/0.4/2.0/3.7	1/2/2/0	4.95±0.98 ^{def}	2257±28 ^b
<i>E. saligna</i>	6 (1/2/3/60)	0.2/0.2/2.0/3.7	1/2/2/0	5.30±0.90 ^{cdef}	2232±40 ^b
Edge-Grain-to-Edge-Grain Joints					
<i>E. saligna</i> *	5 (1/2/2/60)	0.4/0.4/2.0/3.7	0.75/1.5/1.5/0	7.29±1.08 ^b	1501±22 ^h
<i>E. saligna</i> *	6 (1/2/3/60)	0.2/0.2/2.0/3.7	1/2/2/0	6.54±0.56 ^{bcd}	NA
<i>E. saligna</i> †	6 (1/1/4/60)	0.2/0.2/1.8/3.7	1/2/2/0	7.09±1.20 ^b	2036±36 ^{cd}
<i>E. pilularis</i> †	6 (1/1/4/60)	0.2/0.2/1.8/3.7	1/2/2/0	9.45±0.43 ^a	1990±27 ^d
<i>E. pilularis</i> *	6 (1/2/3/60)	0.2/0.2/2.0/3.7	1/2/2/0	7.07±3.12 ^{bc}	1995±45 ^{cd}
<i>C. maculata</i> †	8 (1/1/6/60)	0.2/0.2/1.8/3.7	1/2/2/0	6.15±1.92 ^{bcd}	2476±48 ^a
<i>C. maculata</i> *	8 (1/2/5/60)	0.2/0.2/2.0/3.7	1/2/2/0	6.05±1.49 ^{bcd}	2458±55 ^a
Entries with different superscripts are significantly different from one another ($p < 0.05$); * A welding sequence consisted in two preheating phase substeps to ramp up welding pressure and amplitude, the welding phase and the cooling phase; ** Average Value and Standard deviation; ♣ Parameters used based on butt jointing mechanical property results; † Parameters adapted from Mansouri <i>et al.</i> (2010)					

The average shear strength of joints made with *Eucalyptus saligna* was significantly higher when laminated (*i.e.*, edge-grain-to-edge-grain) as compared to end-jointing while using the same combination of parameters (7.29 and 5.14 MPa, respectively). The results are not surprising considering that end-grain butt joints made with conventional bonding techniques have difficulty meeting the requirements of ordinary service and such joints reach only about 25% of the tensile strength of the wood parallel-to-grain (Frihart and Hunt 2010). The energy consumption during the welding process was also significantly reduced when welding edge-grain-to-edge-grain joints as opposed to end-grain joints dropping from 1774 to 1501 J. The grain orientation also proved to have a significant impact on the mechanical properties of the weldline, as strong joints were generated when using *Eucalyptus pilularis* (9.45±0.43 MPa) and *Corymbia maculata* (6.15±1.92 MPa). Many specimens also presented a high percentage of wood failure. The results suggest that crack development in welded joints is also strongly dependent on the fiber orientation, in which fibers parallel to each other can sustain a WA allowing the weld to sustain the generated thermal stresses as it solidifies.

CONCLUSIONS

1. The present study was initially conducted to define the optimal linear wood welding parameters along the end-grain-to-end-grain faces (*i.e.*, butt joint) for *Eucalyptus saligna*, *Eucalyptus pilularis*, and *Corymbia maculata*. Preliminary trials allowed for the assessment of a wide range of welding pressures (WP), welding amplitudes (WA), and welding times (WT) for optimization purposes. Additional tests were conducted to assess the impact of fiber orientation on the mechanical properties of welded joints.
2. The analysis of end-grain joints made with *Eucalyptus saligna* showed an interaction between WT, WA, and WP specifically during the welding phase. A two-second WT coupled with an extended three-second preheating phase provided significantly stronger joints. As for *Eucalyptus pilularis* and *Corymbia maculata*, all end-grain joints systematically snapped once the holding pressure was removed. This phenomenon suggests that small welded surfaces cannot withstand thermal stresses generated at the weldline as the molten matrix solidifies. Such findings may have implications for future applications, as a welded surface has never been identified as a potential limiting factor before. The behavior of the matrix of molten material would need to be further investigated, as it appears to be dependent on the fiber orientation as well.
3. The grain orientation has a significant impact on the mechanical properties of the weldline. This was demonstrated by the capacity of *Eucalyptus pilularis* and *Corymbia maculata* to generate very strong laminated joints, while that of *Eucalyptus saligna* improved significantly when compared with its end-grain joint counterpart.
4. Energy efficient combinations were generally those involving low WAs and short WTs where WPs had a negligible effect on energy consumption. Measuring the energy consumption also appears as an accurate non-destructive method to assess produced welds as measures of energy consumption are closely related with the mechanical testing results.

5. Welded components could meet standard use requirements throughout its lifetime by using a simple tongue and groove joint. Linear wood welding can, therefore, be used for eco-conception of indoor appearance applications such as flooring overlay, with all three species satisfying both visual and mechanical properties criteria.

ACKNOWLEDGEMENTS

The authors acknowledge the financial support of the University of Melbourne. Thanks are extended to Boral Timber for providing the material.

REFERENCES CITED

- Belleville, B., Ozarska, B., and Pizzi, A. (2016). "Assessing the potential of wood welding for Australian eucalypts and tropical species," *Eur. J. Wood Prod.* 74, 753-757. DOI: 10.1007/s00107-016-1067-5
- Frihart, C. R., and Hunt, C. G. (2010). "Adhesives with wood materials – Bond formation and performance," in: *Wood Handbook – Wood as an Engineering Material*, U.S. Department of Agriculture, Forest Products Laboratory, Madison, WI, pp. 1-24.
- Gfeller, B., Zanetti, M., Properzi, M., Pizzi, A., Pichelin, F., Lehmann, M., and Delmotte, L. (2003). "Wood bonding by vibrational welding," *J. Adhes. Sci. Technol.* 17(11), 1573-1589. DOI: 10.1163/156856103769207419
- Haboudou, A., Peyre, P., and Vannes, A. B. (2003). "Study of keyhole and melt pool oscillations in dual beam welding of aluminium alloys: Effect on porosity formation," *Proceedings of the Society of Photo-optical Instrumentation Engineers (SPIE)* 4831, 295-300. DOI: 10.1117/12.503131
- InsideWood. (2004-onwards). "Wood anatomical database," <http://insidewood.lib.ncsu.edu/search> [Accessed 7 December 2016].
- Mansouri, H. R., Pizzi, A., and Leban, J.-M. (2010). "End-grain butt joints obtained by friction welding of high density eucalyptus wood," *Wood Sci. Technol.* 44, 399-406. DOI: 10.1007/s00226-010-0349-z
- Martins, S. A., Ganier, T., Pizzi, A., and Del Menezzi, C. H. S. (2013). "Parameter scanning for linear welding of Brazilian *Eucalyptus benthamii* wood," *Eur. J. Wood Prod.* 71, 525-527. DOI: 10.1007/s00107-013-0696-1
- The Welding Institute (TWI) (1999). "Defects - solidification cracking," (<http://www.twi-global.com/technical-knowledge/job-knowledge/defects-solidification-cracking-044/>), Accessed 8 August 2016.
- Zhang, H., Pizzi, A., and Xiaoning, L. (2014). "Palmyra palm bonding by vibrational welding," *Eur. J. Wood Prod.* 72, 693-695. DOI: 10.1007/s00107-014-0825-5
- Zhou, J., and Tsai, H.-L. (2007). "Effects of electromagnetic force on melt flow and porosity prevention in pulsed laser keyhole welding," *Int. J. Heat Mass Tran.* 50, 2217-2235. DOI: 10.1016/j.ijheatmasstransfer.2006.10.040

Article submitted: September 21, 2016; Peer review completed: November 21, 2016;
Revised version received: December 7, 2016; Accepted: December 8, 2016; Published:
December 13, 2016.

DOI: 10.15376/biores.12.1.1007-1014